THE JOURNAL OF PHYSICAL CHEMISTRY A

Article

pubs.acs.org/JPCA

TD-CI Simulation of the Strong-Field Ionization of Polyenes

Jason A. Sonk and H. Bernhard Schlegel*

Department of Chemistry, Wayne State University, Detroit, Michigan 48202, United States

ABSTRACT: Ionization of ethylene, butadiene, hexatriene, and octatetraene by short, intense laser pulses was simulated using the time-dependent single-excitation configuration-interaction (TD-CIS) method and Klamroth's heuristic model for ionization (*J. Chem. Phys.* **2009**, *131*, 114304). The calculations used the 6-31G(d,p) basis set augmented with up to three sets of diffuse sp functions on each heavy atom as well as the 6-311++G(2df,2pd) basis set. The simulations employed a seven-cycle cosine pulse (ω = 0.06 au, 760 nm) with intensities up to 3.5×10^{14} W cm^{-2} (E_{max} = 0.10 au) directed along the vector connecting the end carbons of the linear polyenes. TD-CIS simulations for ionization were carried out as a function of the escape distance parameter, the field strength, the number of states, and the basis set size. With a distance parameter of 1 bohr, calculations with Klamroth's heuristic model reproduce the expected trend that the ionization rate increases as the molecular length increases. While the ionization rates are too high at low intensities, the ratios of ionization rates for ethylene, butadiene, hexatriene, and octatetraene are in good agreement with the ratios obtained from the ADK model. As compared to earlier work on the optical response of polyenes to intense laser pulses, ionization using Klamroth's model is less sensitive to the number of diffuse functions in the basis set, and only a fraction of the total possible CIS states are needed to model the strong field ionizations.

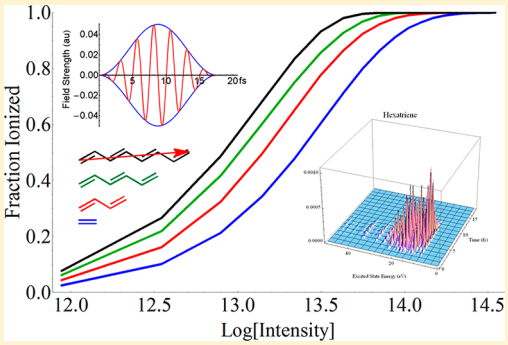

INTRODUCTION

Strong field chemistry encompasses the study of interactions between atoms/molecules and intense laser pulses. The strength of the electric field of these laser pulses is comparable to the electric field sampled by valence electrons. A variety of effects can be observed as a result of these interactions (for recent advances, see refs 1−3). Because the electric field of the laser field approaches that of the field binding the valence electrons, the interactions of the electrons with the field cannot be treated perturbatively. Numerical simulations are needed to model the nonlinear behavior of the electron density. In this Article, we examine the behavior of a series of polyenes subject to a short, intense 760 nm laser pulse. With increasing length and degree of conjugation, the ionization rates of these systems change considerably.[4−8] Time-dependent configuration interaction and the heuristic model of Klamroth and co-workers[9] are used to examine the trends in ionization rates for ethylene, butadiene, hexatriene, and octatetraene.

The electron dynamics of a few electron atoms and diatomics, such as H_2^+ and H_2, have been successfully modeled using highly accurate methods (see refs 10,11, and references therein). These methods, however, cannot readily be used to study the electron dynamics of larger, many electron systems. Two approximate methods are available for many-electron systems: (1) real time integration of the time-dependent Hartree−Fock or density functional equations (rt-TD-HF and rt-TD-DFT methods)[12−16] and (2) time-dependent configuration interaction (TD-CI). Previously, we have used time-dependent Hartree−Fock and TD-CIS methods to simulate the response of CO_2, polyenes, and polyacenes and their cations to short, intense laser pulses.[17−23] Klamroth, Saalfrank, and co-workers[9,24−33] have used TD-CI to study dipole switching, pulse shaping, ionization, dephasing, and dissipation. In the present work, we choose to use the TD-CIS approach to simulate the ionization of a series of polyenes.

Our earlier studies[18] on linear polyenes examined the electronic excitation of conjugated molecules by short, intense laser pulses. The amount of nonadiabatic excitation was found to increase with the length of the polyene. In recent studies,[23,34] we have looked at the number of excited states and the size of the basis set needed in TD-CIS simulations to describe the excited-state populations after the laser pulse. We found that a large number of states (∼300−500) and a basis set augmented with three sets of diffuse functions were needed to model the response to the laser pulse. These studies did not examine ionization. For few-electron systems, grid-based methods with absorbing boundary conditions can be used to calculate accurate ionization rates.[35−37] Mukamel[38,39] and co-workers have simulated π electron dynamics in octatetraene with a semiempirical Hamiltonian and have modeled ionization saturation intensities in a multielectron system in a finite one-dimensional box. For larger systems, Klamroth and co-workers[9] have developed a heuristic approach to model ionization using TD-CI and standard atom centered Gaussian basis sets. For states above the ionization potential, the ionization rate is assumed to be proportional to the speed of the excited electron

Received: March 12, 2012
Revised: May 17, 2012
Published: June 4, 2012

   dx.doi.org/10.1021/jp302389a | *J. Phys. Chem. A* 2012, 116, 7161−7168

Table 1. Linear Polyenes Used in the Current Study, Their Experimentally Determined Ionization Potentials, Total Number of CIS Excited States, and Maximum Number of States Used in the Current Study

		total number of CIS states for the 6-31 *n*+ G(d,p) basis			maximum number of excited states used for 6-31 *n*+ G(d,p)		
	experimental ionization potential (eV)	*n* = 1	*n* = 2	*n* = 3	*n* = 1	*n* = 2	*n* = 3
ethylene	10.5138[45]	288	336	378	288	336	378
butadiene	9.072[45]	957	1111	1254	957	999	999
hexatriene	8.42[46]	2016	2320	2592	999	999	999
octatetraene	7.79[47]	3465	3969	4431	800	800	800

divided by a characteristic escape distance. This model is appropriate in the high field case where above-threshold ionization is dominant. Our goal is to see how well this model applies to the ionization rates of a series of linear polyenes and to examine the effect of the basis set size, number of states, and escape distance parameter on the ionization rates.

METHODS

The time-dependent Schrödinger equation (TDSE) in atomic units is

$$i\frac{d\Psi(t)}{dt} = \hat{H}(t)\Psi(t) \tag{1}$$

The wave function can be expanded in terms of the ground state $|\varphi_0\rangle$ and excited states $|\varphi_i\rangle$ of the time-independent, field-free Hamiltonian.

$$\Psi(t) = \sum_{s=0}^{n} C_s(t)|\psi_s\rangle \tag{2}$$

For the full solution of the TDSE, the sum in eq 2 extends over all bound states and the continuum. For practical applications, the sum needs to be restricted to a suitable subset of states. In the present work, we include only the ground state and the singly excited states.

$$\psi_s^{\mathrm{CIS}} = \sum_{i,a} a_i^a(s)\varphi_i^a \tag{3}$$

The amplitudes, $a_i^a(s)$, and excitation energies, ω_s, are obtained by diagonalizing the corresponding field-free Hamiltonian matrix of the time-independent Schrodinger equation.

$$\hat{H}_0|\psi_s\rangle = \omega_s|\psi_s\rangle,\ \langle\psi_r|\psi_s\rangle = \delta_{rs} \tag{4}$$

Inserting eq 2 into eq 1 and multiplying from the left by $\langle\varphi_i|$ reduces the time-dependent Schrödinger equation to a set of coupled differential equations for the time-dependent coefficients:

$$i\frac{dC_r(t)}{dt} = \sum_s H_{rs}(t)C_s(t) \tag{5}$$

This can be integrated numerically using a unitary transform approach:

$$\mathbf{C}(t + \Delta t) = \exp[-i\mathbf{H}(t + \Delta t/2)\Delta t]\mathbf{C}(t) \tag{6}$$

In the dipole approximation, the matrix elements of the field-dependent Hamiltonian in eqs 5 and 6 can be expressed in terms of the field-free energies, ω_s, transition dipole moments, $\mathbf{D}_{rs}$, and the electric field, $\mathbf{e}(t)$:

$$H_{rs}(t) = \langle\psi_r|\hat{H}(t)|\psi_s\rangle = \langle\psi_r|\hat{H}_0|\psi_s\rangle + \langle\psi_r|\hat{r}|\psi_s\rangle\cdot\mathbf{e}(t)$$
$$= \omega_s\delta_{rs} + \mathbf{D}_{rs}\cdot\mathbf{e}(t) \tag{7}$$

Practical considerations limit the total number of states that can be used. Increasing the number of states included until no further change is seen in the simulation is one means of determining whether the number of states is adequate.

Typical molecular electronic structure calculations use atom centered basis functions. Because continuum functions are not usually included in these calculations, the TD-CI simulations cannot model ionization directly. Klamroth and co-workers[9] formulated a heuristic method to model ionization. For states above the ionization potential (IP), the energy is modified by adding an imaginary component (i/2) Γ_n to the excited-state energy, where Γ_n is the estimated ionization rate for that excited state.

$$\omega_s \rightarrow \omega_s - \frac{i}{2}\Gamma_s \tag{8}$$

In the following calculations, the Γ_n term was added to states above the experimental IPs listed in Table 1. Vertical IPs calculated by UHF and Koopman's theorem are ca. 1.1 and 0.2 eV lower, respectively; nevertheless, the results using the UHF IPs are similar to those obtained with the experimental IPs. The ionization rate, Γ_n, for a state is obtained by summing contributions from the excited determinants that form the excited state. The ionization rate for an electron in an excited determinant is estimated from the velocity of the electron in the virtual orbital divided by an escape distance parameter, *d*. In turn, the velocity of the electron is proportional to the square root of its orbital energy, ε_a.

$$\Gamma_s = \sum_{i,a} |a_i^a(s)|^2 \frac{\sqrt{\varepsilon_a}}{d} \tag{9}$$

where $|a_i^a(s)|^2$ is the probability amplitude for the determinant involving an excitation from orbital *i* to orbital *a* describing state *s*.

The present study uses a linearly polarized and spatially homogeneous external field:

$$\mathbf{e}(r, t) \approx \mathbf{E}(t)\sin(\omega t + \varphi) \tag{10}$$

This is a good approximation for the laser field, because typical wavelengths are much larger than molecular dimensions. The present simulations use a cosine envelope for the laser pulse.

$$g(t) = 1/2 + \cos[2\pi t/(n\tau)]/2 \tag{11}$$

$$\mathbf{E}(t) = \mathbf{E}_{\max}g(t - n\tau/2) \quad \text{for} 0 \le t \le nt$$
$$\mathbf{E}(t) = 0 \quad \text{for} t < 0 \text{and} t > nt \tag{12}$$

where $\tau = 2\pi/\omega$ is the period and *n* is the number of cycles.

dx.doi.org/10.1021/jp302389a | J. Phys. Chem. A 2012, 116, 7161−7168

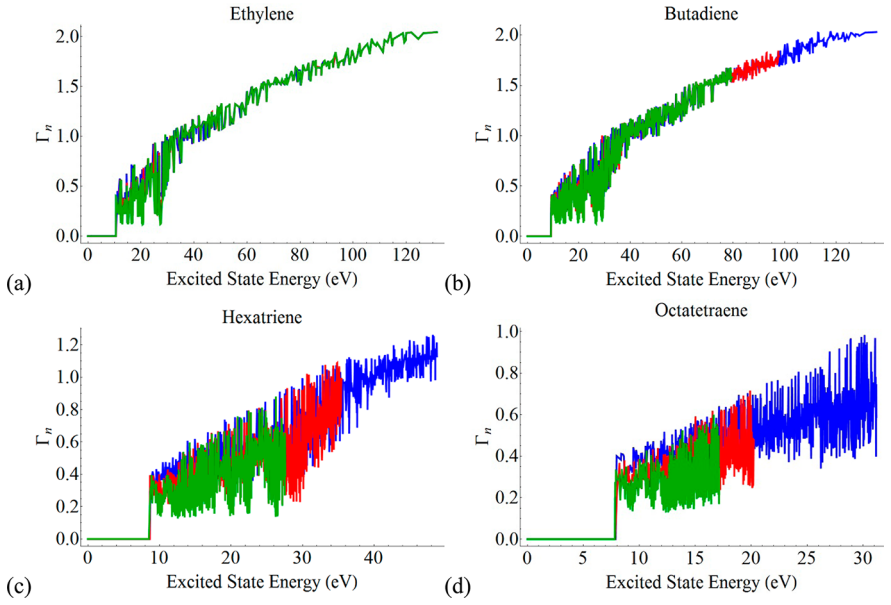

Figure 1. Ionization rates for the excited states of (a) ethylene, (b) butadiene, (c) hexatriene, and (d) octatetraene, using the 6-31 1+ G(d,p) (blue), 6-31 2+ G(d,p) (red), and 6-31 3+ G(d,p) (green) basis sets and a distance parameter of d = 1 bohr in eq 9.

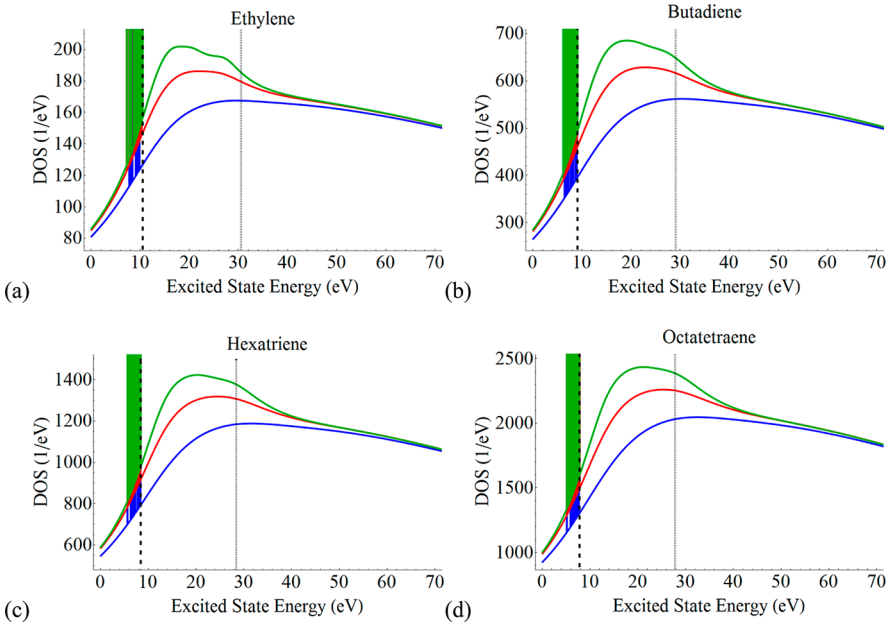

Figure 2. Density of states for (a) ethylene, (b) butadiene, (c) hexatriene, and (d) octatetraene, found using the 6-31 1+ G(d,p) (blue), 6-31 2+ G(d,p) (red), and 6-31 3+ G(d,p) (green) basis sets, all CIS excited states, and a distance parameter d = 1 bohr.

The CIS calculations were carried out with the development version of the Gaussian software package.[40] For this study ethylene, *trans* 1,3-butadienene, all *trans* 1,3,5-hexatriene, and all *trans* 1,3,5,7-octatetraene were optimized at the HF/6-31G(d,p) level of theory. Excited-state calculations were carried out with the 6-31 *n*+ G(d,p) basis set. The 6-31 *n*+ G(d,p) basis has one set of five d functions on the carbons, one set of p functions on the hydrogens, and *n* sets of diffuse s and p functions on all carbons (n = 1, 2, and 3, with exponents of 0.04380, 0.01095, 0.0027375). Some additional calculations were carried out with the 6-311++G(2df,2pd) basis set. A seven-cycle cosine pulse with ω = 0.06 au (760 nm) was used in the simulations. The length of the pulse is about 18 fs, and the simulation is allowed to run for an additional 6 fs after the pulse. For maximal effect, the field was directed along the long axis of the molecule, specifically along the vector connecting the end carbons. Practical considerations in the calculation of excited to excited-state transition dipoles limited the simulations to ca. 1000 states for butadiene and hexatriene, and 800 states for octatetraene. The total number of singly excited states and the maximum number of states used in the simulations for each molecule are listed in Table 1. Mathematica[41] was used to integrate the TD-CI equations and analyze the results. The TD-CI integrations were carried out with a step size of 0.05 au (1.2 as).

dx.doi.org/10.1021/jp302389a | J. Phys. Chem. A 2012, 116, 7161−7168

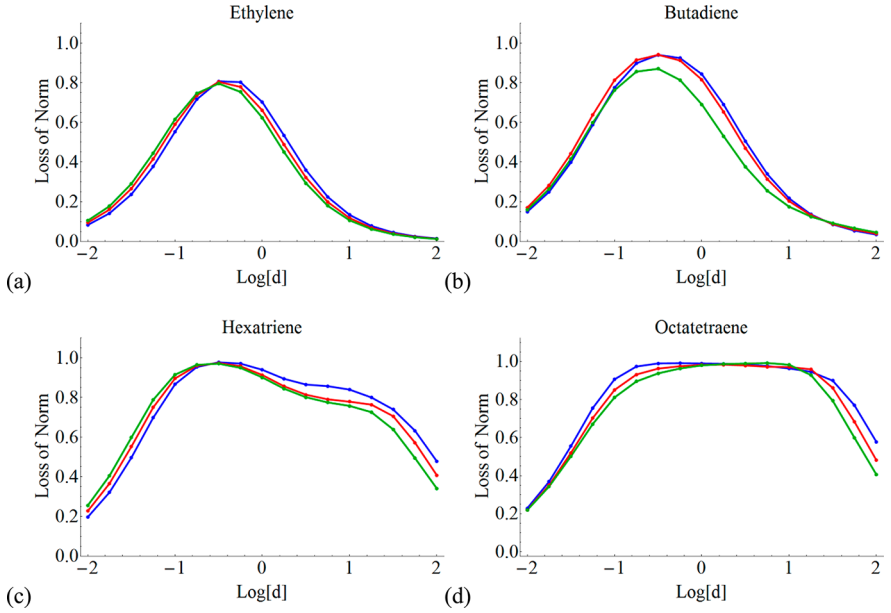

Figure 3. Loss of norm as a function of the distance parameter d (in bohr) for (a) ethylene, (b) butadiene, (c) hexatriene, and (d) octatetraene, using the 6-31 1+ G(d,p) (blue), 6-31 2+ G(d,p) (red), and 6-31 3+ G(d,p) (green) basis sets for E_{max} = 0.05 au.

RESULTS AND DISCUSSION

In earlier studies,[23] we examined various levels of theory and basis sets to help determine what one should consider when simulating the response of a molecule to an intense laser pulse. For systems that cannot directly model ionization, TD-CIS calculations of butadiene needed up to 500 excited states computed with the 6-31G(d,p) basis set with three additional sets of diffuse sp functions to describe the optical response to a three-cycle, 760 nm pulse with an intensity of ca. 10^{14} W cm^{-2}. In a similar vein, this Article looks at the effect of basis set size and the number of states on the ionization rate of a set of linear polyenes using Klamroth's heuristic model.

Table 1 lists the linear polyenes used in the present study, along with their experimentally determined ionization potentials. Also indicated in the table are the total number of singly excited states available for a given basis set and the maximum number used in the simulations. The excited-state ionization rates, Γ_n, computed with eq 9 and an escape distance parameter of d = 1 bohr are shown in Figure 1 for ethylene, butadiene, hexatriene, and octatetraene. The general trend is Γ_n increases as the energies of the states increase, but there are large fluctuations in the value of Γ_n. The higher energy states usually involve excitation to higher energy virtual orbitals, which result in larger values of Γ_n. However, some of the higher excited states involve excitations from low lying occupied orbitals to low lying virtual orbitals, yielding smaller values of Γ_n. Larger basis sets generate more states at lower energy and more low values of Γ_n. Changing the distance parameter shifts these curves up or down by the appropriate factor, but does not change the shape of the plots.

The ionization rate or lifetime of the excited states leads to a broadening of the excited-state energies. The energy can be represented by a normalized Lorentzian with a width of Γ_n. Summing over all of the CIS states for a given basis set yields the density of states plots shown in Figure 2 for a distance parameter d = 1 bohr. The blue, green, and red curves correspond to n = 1, 2, 3 for the 6-31 n+ G(d,p) basis. The vertical dashed lines indicate the ionization potential, and the solid vertical lines are drawn at 20 eV above the ionization potential. For higher energies, the density of states converges nicely into a broad continuum-like feature for all three basis sets for each molecule. Increasing the number of diffuse functions from n = 1 to n = 3 primarily affects the states within ca. 20 eV of the ionization potential and corresponds to an increasing number of low-lying pseudocontinuum states. For a distance parameter of d = 10 bohr (not shown), the widths of the states are reduced by a factor of 10, and more structure is seen in the 10−30 eV range. As in the d = 1 bohr case, the density of states at higher energies for d = 10 is the same for 1, 2, and 3 sets of diffuse functions.

In the heuristic model, the ionization rate depends on three factors. The probability amplitude and the molecular orbital energies are determined by the calculation, but the escape distance parameter d must be determined empirically. The ionization rate Γ_n depends inversely on d. Klamroth and co-workers found the loss of norm of their systems reached a maximum near d = 1. Figure 3 shows the loss of norm of the population as a function of d for the four linear polyenes with each of the 6-31 n+ G(d,p) basis sets using the maximum number of states listed in Table 1. For ethylene, the peak in the loss of norm is near d = 1. For the longer polyenes, the peak becomes broader, extending to larger values of d, corresponding to smaller values of Γ_n.

The trends in Figure 3 can be understood by using perturbation theory to describe the time-dependent behavior of a simple two-state problem. Let the lower state have an energy of 0, the upper state an energy of $\omega - i\Gamma/2$. If a perturbation causes the states to interact, the loss of population depends on $\mathrm{Im}(1/(\omega - i\Gamma/2)) = (\Gamma/2)/(\omega^2 + (\Gamma/2)^2)$ as well as on the magnitude of the perturbation. The loss of population is proportional to Γ for small values of Γ, reaches maximum for $\Gamma/2 = \omega$, and goes to zero for large Γ. Thus, the maximum ionization rate for given state occurs when $\Gamma_n/2$ is equal to the excitation energy of the state. Ethylene has relatively few states that interact with the ground state under the influence of the laser field, and strong ionization occurs near d = 1. For longer polyenes, there are more states that interact with the ground

dx.doi.org/10.1021/jp302389a | J. Phys. Chem. A 2012, 116, 7161−7168

state. Because these states are lower in energy for longer polyenes, smaller values of Γ_n and hence larger values of d will also cause strong ionization. Because all of the polyenes ionize strongly for d = 1, this is the primary value used for additional analyses.

Figure 4 shows the seven-cycle 760 nm cosine pulse and the time evolution of the norm of the wave functions for ethylene, butadiene, hexatriene, and octatetraene during the pulse. The norm of ethylene decreases the least, reaching ca. 0.30 by the end of the pulse, while the norm for octatetraene decreases nearly to zero just after the maximum in the pulse. The instantaneous ionization rate shown in Figure 4c can be obtained from the derivative of the norm with respect to time. Alternatively, the instantaneous ionization rate can be calculated by multiplying the value of Γ_n for a state by its population and summing over all of the states. Early in the pulse, when the intensities are low, it is already apparent that the ionization rate is greatest for octatetraene and least for ethylene. Toward the end of the pulse, the ionization rate for ethylene is still significant, whereas the rate for octatetraene is nearly zero. This reversal of the trend in the instantaneous rates is because the population of octatetraene is very small during the last few cycles of the pulse but the population of ethylene is still fairly large.

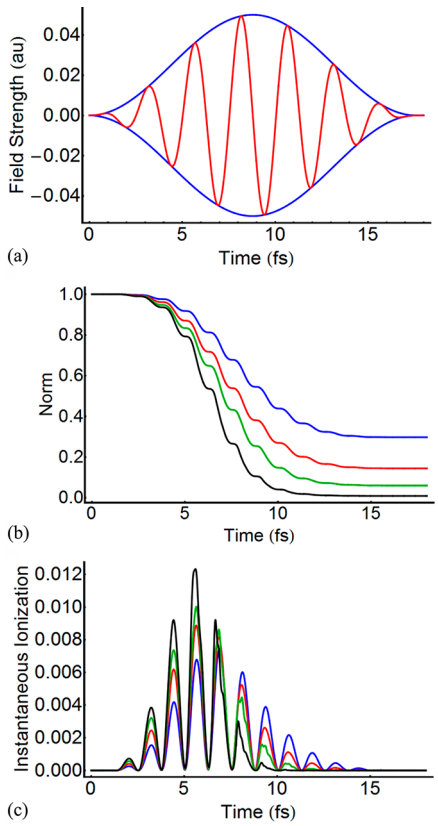

Figure 4. (a) Electric field for a seven-cycle 760 nm cosine pulse with intensity of 0.88×10^{14} W cm^{-2} (E_{max} = 0.05 au), (b) time evolution of the wave function norm during the pulse, and (c) instantaneous ionization rate for ethylene (blue), butadiene (red), hexatriene (green), and octatetraene (black) with a distance parameter d = 1 bohr using the 6-31 1+ G(d,p) basis set.

Inspection of the ionization rates for the individual states provides some insight into the dependence of the total ionization rate on the escape distance parameter. Instantaneous ionization rates for ethylene and hexatriene are shown in Figure 5 as a function of state energy and time. As expected, the populations of the excited states and hence ionization rates for these states peak when the laser field peaks and the polarization of the electronic distribution is the greatest. For each of the polyenes, the ionization is dominated by a relatively small number of excited states in the range of 0− 20 eV above the IP. There are many more states in this range that contribute only weakly to the ionization but are needed to treat the polarization of the electron cloud in the simulation. Even for calculations of the static polarizability in the sum-over-states formalism, states up to 20 eV above the IP are needed to get within 3% of the correct values.

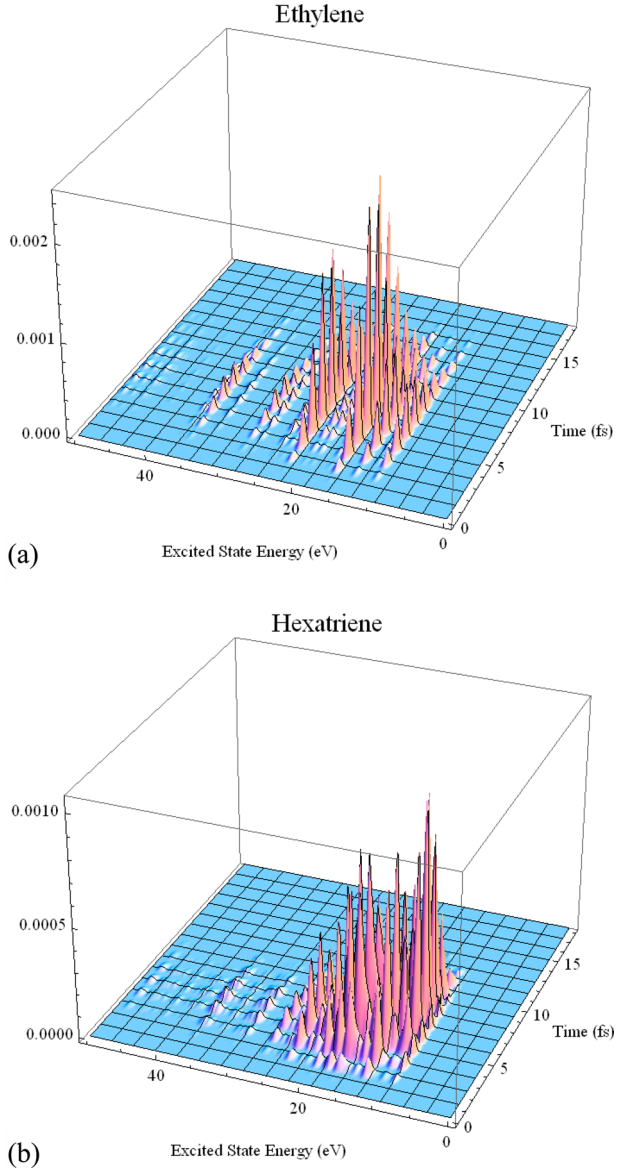

Figure 5. Instantaneous ionization rates as a function of state number and time for (a) ethylene and (b) hexatriene. The simulations used a seven-cycle 760 nm cosine pulse with E_{max} = 0.05 atomic units, and employed a distance parameter d = 1 bohr, 288 excited states for ethylene, and 999 excited states for hexatriene computed with the 6-31 1+ G(d,p) basis.

dx.doi.org/10.1021/jp302389a | J. Phys. Chem. A 2012, 116, 7161−7168

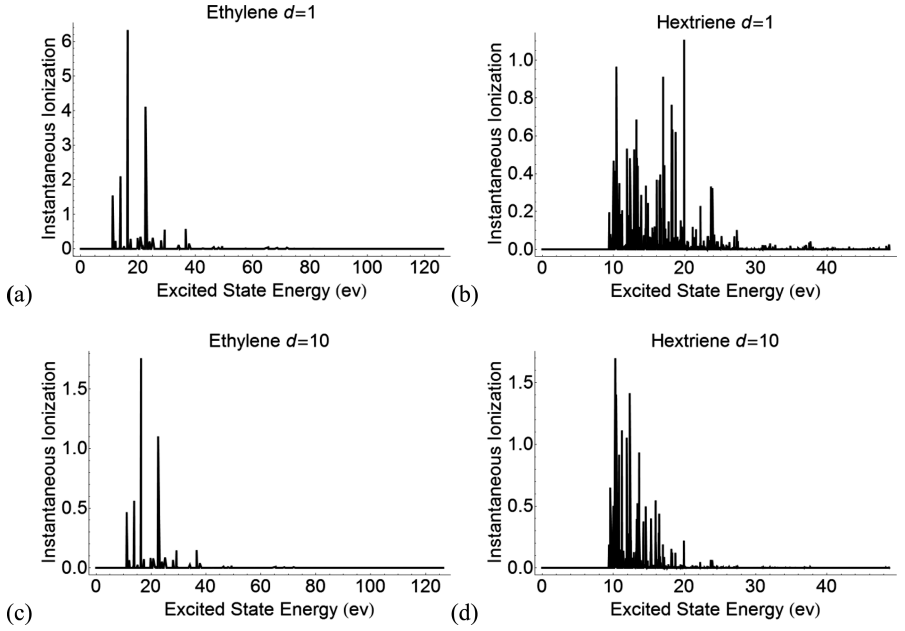

Figure 6. Contributions of individual states to the loss of norm for (a) ethylene with escape distance parameter d = 1 bohr, (b) hexatriene with d = 1 bohr, (c) ethylene with d = 10 bohr, and (d) hexatriene with d = 10 bohr. The simulations used a seven-cycle 760 nm cosine pulse with E_{max} = 0.05 atomic units, and employed 288 excited states for ethylene and 999 excited states for hexatriene computed with the 6-31 1+ G(d,p) basis.

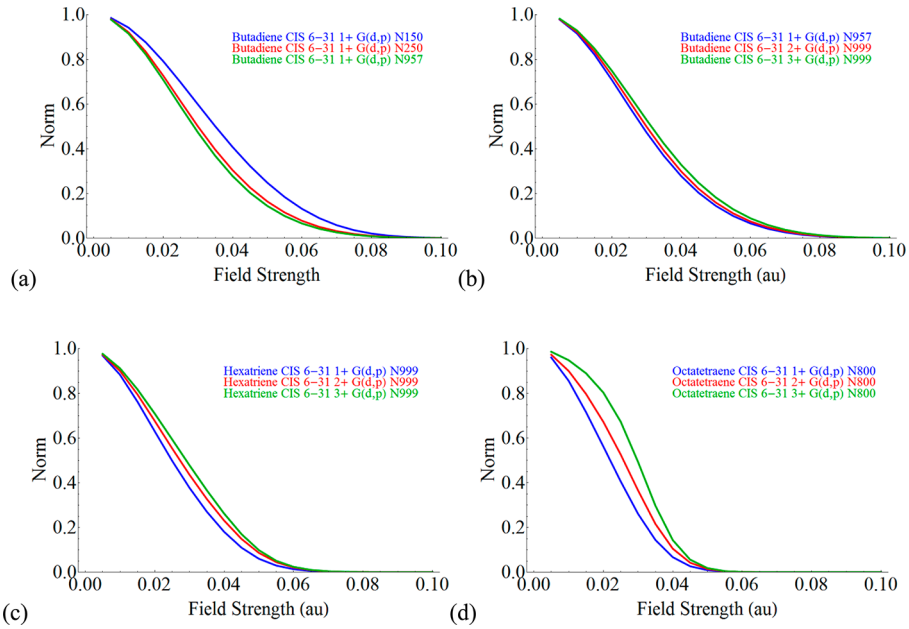

Figure 7. Effect of basis set size and number of states on the wave function norm after the pulse as a function of field strength for (a) butadiene with the 6-31 1+ G(d,p) basis set and 150 states (blue), 250 states (red), and all 957 CIS excited states (green), (b) butadiene, (c) hexatriene, and (d) octatetraene with 6-31 1+ G(d,p), 6-31 2+ G(d,p), and 6-31 3+ G(d,p) basis sets (blue, red, and green, respectively) with d = 1 bohr.

The contribution of an individual state to the total ionization can be obtained by integrating its instantaneous ionization rate over the duration of the pulse. Figure 6 compares the results for d = 1 and d = 10 bohr for ethylene and hexatriene. For ethylene, the same states contribute to the total ionization d = 1 and d = 10 bohr. The values are smaller for the latter but the ratios are nearly the same. In the case of hexatriene, many states in the 10−30 eV range are involved in the ionization process for d = 1 bohr. For d = 10 bohr, the distribution is shifted toward lower energies, and the contributions from these states are larger than for d = 1. This is in keeping with the analysis of the two-state system discussed above. A larger value of d yields smaller Γ's. Because the maximum ionization rate occurs when $\omega = \Gamma/2$, lower energy states contribute more when the Γ's are smaller. Because hexatriene and octatetraene have more low energy states than ethylene and butadiene, ionization as a function of the escape distance d, shown in Figure 3, is much broader for the longer polyenes.

Figure 7 shows the calculated loss of norm of the TD-CIS wave function for each of the linear polyenes after a seven-cycle 760 nm cosine pulse with intensities up to 3.51×10^{14} W cm^{-2} (field strengths up to 0.10 au) for a distance parameter of d = 1

dx.doi.org/10.1021/jp302389a | J. Phys. Chem. A 2012, 116, 7161−7168

bohr. The effect of varying the number of states used in the simulation is examined in Figure 7a for butadiene with the 6-31 1+ G(d,p) basis set. As compared to the results with all 957 CIS excited states, the norm of wave function after the laser pulse is well represented with as few as 250 states. This corresponds to including all states that are within 20 eV of the IP. Using only 150 states corresponds to using all of the states up to ∼19.5 eV (only 10.5 eV above the IP); doing so neglects strong contributions toward ionization from states in the 20−30 eV range (10−20 eV above the IP). The overall contributions from a few states in this 20−30 eV range can be quite large as can be seen in Figure 6. Adding more polarization functions (e.g., 6-311++G(2df,2pd) basis) has little effect on the ionization rate of butadiene (not shown). Figure 7b−d shows the effect of diffuse functions on the loss of norm for the polyenes. With ca. 1000 states, the results for butadiene and hexatriene are very similar with 1, 2, and 3 sets of diffuse functions. This indicates that ionization with Klamroth's heuristic model is not as sensitive to diffuse functions as the optical response in the absence of ionization.[23] For octatetraene, some basis set effects can be seen. At low field strengths, the ionization rate diminishes as the number of diffuse functions is increased. However, it is not the presence of diffuse function that decreases the ionization rate, but rather the absence of higher energy states. With the 6-31 *n*+ G(d,p) basis, a choice of 800 states includes all excitations up to 24, 13, and 9 eV above the IP for n = 1, 2, and 3 sets of diffuse functions, respectively (compare with Figure 1d). Adding more diffuse functions increases the number of low energy excited states, thereby decreasing the maximum excitation energy attainable within the lowest 800 states. For the 6-31 3+ basis set, the ionization rate at small field strengths is too low because too few high energy, rapidly ionizing states are included within the set of the 800 states. Nevertheless, for $E_{max} \geq 0.05$ au, all three basis sets yield complete ionization of octatetraene by the seven-cycle 760 nm pulse.

Figure 8 summarizes the ionization of ethylene, butadiene, hexatriene, and octatetraene as a function of the intensity for a seven-cycle 760 nm cosine pulse. At high intensities, each of the polyenes is ionized completely by the pulse. At lower intensities, the fraction ionized is largest for octatetraene and least for ethylene, as could be anticipated qualitatively from the trend in the ionization potentials. Experimental ionization saturation intensities, I_{sat}, have been measured for a number of saturated and unsaturated hydrocarbons. Corkum and co-workers[4,5] were able to determine $I_{sat} = 89 \times 10^{12}$ W cm^{-2} for hexatriene and $I_{sat} = 110 \times 10^{12}$ W cm^{-2} for ethylene. Our calculations yield strong ionizations in the right order of magnitude of intensities: 10^{12}−10^{14} W cm^{-2}. However, it is not possible to compare the computed ionization rates directly with experiment. The distance parameter is empirical and has a large effect on the ionization rate. Only one orientation was used in the calculation rather than averaging over all orientations. The longer polyenes can have several conformations, but the calculations were only for the all-trans conformation. Other variables such as pulse length and shape also affect the degree of ionization.

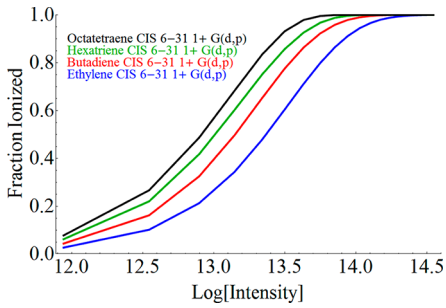

Figure 8. Fraction ionized by the pulse as a function of the intensity (W cm^{-2}) for ethylene (blue), butadiene (red), hexatriene (green), and octatetraene (black) calculated using the 6-31 1+ G(d,p) basis set and d = 1 bohr.

Some of the difficulties associated with comparing the calculations and experiment can be circumvented by examining the ratios of intensities. For our seven-cycle cosine pulse, the field strengths that cause a 50% decrease in the population are 0.026 au for ethylene, 0.020 au for butadiene, 0.017 au for hexatriene, and 0.015 au for octatetraene with the 6-31 1+ G(d,p) basis set and a distance parameter of d = 1 bohr. The ratios of intensities relative to ethylene are 0.61 for butadiene, 0.44 for hexatriene, and 0.35 for octatetraene. Similar ratios are found for 75% decrease in the population and for two and three sets of diffuse functions (except for octatetraene, which would require more states for the TD-CIS simulation with two and three sets of diffuse functions, as noted above). However, the ratio for hexatriene to ethylene is significantly smaller than the ratio of 0.81 for the experimental I_{sat} values. In the present calculations, the molecules are aligned to the laser field, possibly increasing the difference in the ionization rates.

For rare gas atoms and ions, ADK theory[42,43] provides a good description of the dependence of the ionization rate on the ionization potential. It is known, however, that in certain cases ADK theory fails to predict correct saturation intensities for laser pulses at 800 nm and shorter wavelengths because of interference effects.[44] To circumvent these and related limitations of ADK, we compare only the ratios of the ionization rates. The ratios of ionization rates relative to ethylene computed by ADK theory are 0.59 for butadiene, 0.45 for hexatriene, and 0.34 for octatetraene when integrated over the same pulse shape. The ionization rates obtained from the TD-CIS simulations compare very well with these ratios, indicating that the heuristic ionization model recovers the correct trend in dependence of the ionization rates on the ionization potentials. However, the TD-CIS simulations with the heuristic ionization model predict a much slower rise in the fraction ionized as the intensity increases. The heuristic model also leads to a much higher ionization rate at low intensities than expected from ADK. This is likely due to the fact that the heuristic approach assumes an above-threshold model for ionization, whereas ADK is based on tunneling. The heuristic model for ionization in TD-CI simulations depends on only the energies of the virtual orbitals. A more sophisticated model such as complex absorbing potentials would be needed to take into account the shape of the orbitals and the direction of the field.

■ CONCLUSIONS

The heuristic approach developed by Klamroth and co-workers provides a satisfactory method for modeling the trends in ionization rates of short linear polyenes. The ionization rate is sensitive to the escape distance parameter, and a value of d = 1 bohr was found suitable for ethylene, butadiene, hexatriene, and octatetraene. In contrast to earlier work on modeling the optical response of polyenes to an intense pulse, ionization with

Klamroth's model is less sensitive to the basis set size. The 6-31G(d,p) basis set augmented with a single set of diffuse functions on the carbon atoms yields results similar to calculations with three sets of diffuse functions. TD-CIS calculations also depend on the number of excited states used in the simulation. For the pulse parameters considered, consistent results for the ionization of linear polyenes were found using all states up to ca. 20 eV above the IP. Although this method does not yield ionization rates that can be compared directly to experiment, ratios of the calculated ionization rates are in good agreement with the ratios predicted by the ADK model.

AUTHOR INFORMATION

Corresponding Author

*E-mail: hbs@chem.wayne.edu.

Notes

The authors declare no competing financial interest.

ACKNOWLEDGMENTS

This work was supported by a grant from the National Science Foundation (CHE0910858). Wayne State University's computing grid provided computational support. J.A.S. would like to thank the IMSD Program at WSU for financial support (GM058905-11).

REFERENCES

(1) *Strong Field Laser Physics*; Brabec, T., Ed.; Springer: New York, 2008.
(2) *Lectures on Ultrafast Intense Laser Science*; Yamanouchi, K., Ed.; Springer: New York, 2010.
(3) *Progress in Ultrafast Intense Laser Science I-VII*; Springer: Berlin; New York, 2011.
(4) Hankin, S. M.; Villeneuve, D. M.; Corkum, P. B.; Rayner, D. M. *Phys. Rev. Lett.* **2000**, *84*, 5082−5085.
(5) Hankin, S. M.; Villeneuve, D. M.; Corkum, P. B.; Rayner, D. M. *Phys. Rev. A* **2001**, *64*, 013405.
(6) Lezius, M.; Blanchet, V.; Ivanov, M. Y.; Stolow, A. *J. Chem. Phys.* **2002**, *117*, 1575−1588.
(7) Markevitch, A. N.; Romanov, D. A.; Smith, S. M.; Levis, R. J. *Phys. Rev. Lett.* **2004**, *92*, 063001.
(8) Markevitch, A. N.; Romanov, D. A.; Smith, S. M.; Schlegel, H. B.; Ivanov, M. Y.; Levis, R. J. *Phys. Rev. A* **2004**, *69*, 013401.
(9) Klinkusch, S.; Saalfrank, P.; Klamroth, T. *J. Chem. Phys.* **2009**, *131*, 114304.
(10) Schafer, K. J. In *Strong Field Laser Physics*; Brabec, T., Ed.; Springer: New York, 2008; pp 111−145.
(11) Kono, H.; Nakai, K.; Kanno, M.; Sato, Y.; Koseki, S.; Kato, T.; Fujimura, Y. In *Progress in Ultrafast Intense Laser Science*; Toennies, J. P., Yamanouchi, K., Eds.; Springer-Verlag: Berlin, 2008; Vol. *IV*, pp 41−66.
(12) Bertsch, G. F.; Iwata, J. I.; Rubio, A.; Yabana, K. *Phys. Rev. B* **2000**, *62*, 7998−8002.
(13) Isborn, C. M.; Li, X. *J. Chem. Theory Comput.* **2009**, *5*, 2415−2419.
(14) Lopata, K.; Govind, N. *J. Chem. Theory Comput.* **2011**, *7*, 1344−1355.
(15) Yabana, K.; Bertsch, G. F. *Phys. Rev. B* **1996**, *54*, 4484−4487.
(16) Yabana, K.; Bertsch, G. F. *Int. J. Quantum Chem.* **1999**, *75*, 55−66.
(17) Li, X. S.; Smith, S. M.; Markevitch, A. N.; Romanov, D. A.; Levis, R. J.; Schlegel, H. B. *Phys. Chem. Chem. Phys.* **2005**, *7*, 233−239.
(18) Smith, S. M.; Li, X. S.; Markevitch, A. N.; Romanov, D. A.; Levis, R. J.; Schlegel, H. B. *J. Phys. Chem. A* **2005**, *109*, 5176−5185.
(19) Smith, S. M.; Li, X. S.; Markevitch, A. N.; Romanov, D. A.; Levis, R. J.; Schlegel, H. B. *J. Phys. Chem. A* **2005**, *109*, 10527−10534.
(20) Smith, S. M.; Li, X. S.; Markevitch, A. N.; Romanov, D. A.; Levis, R. J.; Schlegel, H. B. *J. Phys. Chem. A* **2007**, *111*, 6920−6932.
(21) Smith, S. M.; Romanov, D. A.; Heck, G.; Schlegel, H. B.; Levis, R. J. *J. Phys. Chem. C* **2010**, *114*, 5645−5651.
(22) Smith, S. M.; Romanov, D. A.; Li, X. S.; Sonk, J. A.; Schlegel, H. B.; Levis, R. J. *J. Phys. Chem. A* **2010**, *114*, 2576−2587.
(23) Sonk, J. A.; Caricato, M.; Schlegel, H. B. *J. Phys. Chem. A* **2011**, *115*, 4678−4690.
(24) Klamroth, T. *J. Chem. Phys.* **2006**, *124*, 144310.
(25) Krause, P.; Klamroth, T. *J. Chem. Phys.* **2008**, *128*, 234307.
(26) Krause, P.; Klamroth, T.; Saalfrank, P. *J. Chem. Phys.* **2005**, *123*, 74105.
(27) Krause, P.; Klamroth, T.; Saalfrank, P. *J. Chem. Phys.* **2007**, *127*, 034107.
(28) Nest, M.; Klamroth, T.; Saalfrank, P. *J. Chem. Phys.* **2005**, *122*, 124102.
(29) Tremblay, J. C.; Klamroth, T.; Saalfrank, P. *J. Chem. Phys.* **2008**, *129*, 084302.
(30) Tremblay, J. C.; Klinkusch, S.; Klamroth, T.; Saalfrank, P. *J. Chem. Phys.* **2011**, *134*, 044311.
(31) Tremblay, J. C.; Krause, P.; Klamroth, T.; Saalfrank, P. *Phys. Rev. A* **2010**, *81*, 063420.
(32) Huber, C.; Klamroth, T. *J. Chem. Phys.* **2011**, *134*, 054113.
(33) Klinkusch, S.; Klamroth, T.; Saalfrank, P. *Phys. Chem. Chem. Phys.* **2009**, *11*, 3875−3884.
(34) Sonk, J. A.; Schlegel, H. B. *J. Phys. Chem. A* **2011**, *115*, 11832−11840.
(35) Riss, U. V.; Meyer, H. D. *J. Phys. B: At. Mol. Opt. Phys.* **1993**, *26*, 4503−4536.
(36) Neuhauser, D.; Baer, M.; Judson, R. S.; Kouri, D. J. *Comput. Phys. Commun.* **1991**, *63*, 460−481.
(37) Muga, J. G.; Palao, J. P.; Navarro, B.; Egusquiza, I. L. *Phys. Rep.* **2004**, *395*, 357−426.
(38) Suzuki, M.; Mukamel, S. *J. Chem. Phys.* **2003**, *119*, 4722−4730.
(39) Suzuki, M.; Mukamel, S. *J. Chem. Phys.* **2004**, *120*, 669−676.
(40) Frisch, M. J.; Trucks, G. W.; Schlegel, H. B.; Scuseria, G. E.; Robb, M. A.; Cheeseman, J. R.; et al. *Gaussian*, revision H.13; Gaussian, Inc.: Wallingford, CT, 2010.
(41) *Mathematica*, 8.0 ed.; Wolfram Research, Inc.: Champaign, IL, 2010.
(42) Ammosov, M. V.; Delone, N. B.; Krainov, V. P. *Sov. Phys. JETP* **1986**, *64*, 1191−1194.
(43) Tong, X. M.; Zhao, Z. X.; Lin, C. D. *Phys. Rev. A* **2002**, *66*, 033402.
(44) Dura, J.; Gruen, A.; Bates, P. K.; Teichmann, S. M.; Ergler, T.; Senftleben, A.; Pfluger, T.; Schroter, C. D.; Moshammer, R.; Ullrich, J.; Jaron-Becker, A.; Becker, A.; Biegert, J. *J. Phys. Chem. A* **2012**, *116*, 2662−2668.
(45) Lias, S. G. Ionization Energy Evaluation. *NIST Chemistry WebBook, NIST Standard Reference Database Number 69*; National Institute of Standards and Technology: Gaithersburg, MD, 2010.
(46) Franklin, J. L.; Carroll, S. R. *J. Am. Chem. Soc.* **1969**, *91*, 6564−6569.
(47) Jones, T. B.; Maier, J. P. *Int. J. Mass Spectrom. Ion Processes* **1979**, *31*, 287−291.